Journal of Cellular Biochemistry 101:498–516 (2007)

Characterization of Liver Disease and Lipid Metabolism in the Niemann-Pick C1 Mouse

William S. Garver,[1]* David Jelinek,[1] Janice N. Oyarzo,[1] James Flynn,[1] Matthew Zuckerman,[1] Kumar Krishnan,[1] Byung H. Chung,[2] and Randall A. Heidenreich[1]

[1]Department of Pediatrics, The University of Arizona, Tucson, Arizona
[2]Department of Medicine, University of Alabama, Birmingham, Alabama

Abstract Niemann-Pick type C1 (NPC1) disease is an autosomal-recessive cholesterol-storage disorder characterized by liver dysfunction, hepatosplenomegaly, and progressive neurodegeneration. The NPC1 gene is expressed in every tissue of the body, with liver expressing the highest amounts of NPC1 mRNA and protein. A number of studies have now indicated that the NPC1 protein regulates the transport of cholesterol from late endosomes/lysosomes to other cellular compartments involved in maintaining intracellular cholesterol homeostasis. The present study characterizes liver disease and lipid metabolism in NPC1 mice at 35 days of age before the development of weight loss and neurological symptoms. At this age, homozygous affected ($NPC1^{-/-}$) mice were characterized with mild hepatomegaly, an elevation of liver enzymes, and an accumulation of liver cholesterol approximately four times that measured in normal ($NPC1^{+/+}$) mice. In contrast, heterozygous ($NPC1^{+/-}$) mice were without hepatomegaly and an elevation of liver enzymes, but the livers had a significant accumulation of triacylglycerol. With respect to apolipoprotein and lipoprotein metabolism, the results indicated only minor alterations in $NPC1^{-/-}$ mouse serum. Finally, compared to $NPC1^{+/+}$ mouse livers, the amount and processing of SREBP-1 and -2 proteins were significantly increased in $NPC1^{-/-}$ mouse livers, suggesting a relative deficiency of cholesterol at the metabolically active pool of cholesterol located at the endoplasmic reticulum. The results from this study further support the hypothesis that an accumulation of lipoprotein-derived cholesterol within late endosomes/lysosomes, in addition to altered intracellular cholesterol homeostasis, has a key role in the biochemical and cellular pathophysiology associated with NPC1 liver disease. J. Cell. Biochem. 101: 498–516, 2007.

Key words: cholesterol; lipid metabolism; liver disease; Niemann-Pick C1

Niemann-Pick type C1 (NPC1) disease is an autosomal-recessive cholesterol-storage disorder characterized by liver dysfunction, hepatosplenomegaly, and progressive neurodegeneration [Patterson et al., 2001]. The gene responsible for NPC1 disease has been identified in both humans and mice, with the encoded protein designated as the Niemann-Pick C1 (NPC1) protein [Carstea et al., 1997; Loftus et al., 1997]. The predicted amino acid sequence of NPC1 contains a number of structural motifs including (i) a signal-peptide at the amino-terminus for endoplasmic reticulum insertion, (ii) a highly conserved cysteine-rich region with a leucine zipper referred to as the NPC1 domain, (iii) five transmembrane domains comprising a sterol-sensing domain homologous to other proteins involved in regulating cholesterol metabolism, and (iv) a dileucine motif at the carboxyl-terminus that mediates targeting of proteins to late endosomes/lysosomes [Watari et al., 1999; Davies and Ioannou, 2000]. Mutational analysis of the NPC1 gene has revealed that mutations residing within the NPC1 domain and sterol-sensing domain are particularly deleterious towards function of the NPC1 protein [Sun et al., 2001; Park et al., 2003].

At the cellular level, NPC1 disease is characterized by an accumulation of cholesterol in late endosomes/lysosomes derived from endocytosis of lipoproteins through the coated-pit pathway [Pentchev et al., 1985; Liscum et al., 1989; Xie et al., 1999a]. These findings include

Grant sponsor: Ara Parseghian Medical Research Foundation; Grant sponsor: National Institutes of Health; Grant number: R21-DK071544-01.

*Correspondence to: William S. Garver, Department of Pediatrics, Arizona Health Sciences Center, The University of Arizona, 1501 N. Campbell Avenue, Tucson, Arizona 85724. E-mail: wgarver@peds.arizona.edu

Received 20 February 2006; Accepted 14 October 2006
DOI 10.1002/jcb.21200

cells of the central nervous system, whereby cholesterol-containing particles secreted from glial cells are internalized into neurons by the low density lipoprotein receptor (LDLR) and LDLR-related protein (LRP) resulting in the accumulation of cholesterol in late endosomes/lysosomes [Xie et al., 2000a; Dietschy and Turley, 2004; Li et al., 2005]. As such, it is now generally believed that the NPC1 protein regulates the transport of cholesterol from late endosomes/lysosomes to other cellular compartments, specifically the Golgi apparatus, plasma membrane, and endoplasmic reticulum [Blanchette-Mackie et al., 1988; Liscum et al., 1989; Garver et al., 2002; Wojtanik and Liscum, 2003]. Consistent with this function, studies performed in human and mouse fibroblasts have demonstrated that the NPC1 protein is primarily localized to novel vesicles that transiently interact with cholesterol-enriched late endosomes/lysosomes [Neufeld et al., 1999; Garver et al., 2000]. Moreover, with respect to the NPC1 protein having a role in transporting cholesterol to the plasma membrane, recent studies have determined that apolipoprotein A-I (apoA-I)-mediated cholesterol efflux facilitated by the ATP-binding cassette A1 (ABCA1) transporter is impaired in human and mouse NPC1 cells [Chen et al., 2001; Choi et al., 2003].

A mouse model for NPC1 disease, the BALB/cJ *Npc1*^{NIH} (NPC1) mouse, has been shown to closely resemble human NPC1 disease and is used to investigate in vivo aspects of this disorder [Pentchev et al., 1980, 1984, 1986]. One of the first studies performed using the NPC1 mouse demonstrated that a high-cholesterol diet increased the concentration of cholesterol in the liver and induced hepatomegaly, compared to normal littermates [Pentchev et al., 1980, 1984]. Shortly thereafter, a series of eloquent studies determined that the accumulation of cholesterol in the NPC1 mouse expanded continuously from birth, particularly in the liver, and was proportional to the rate at which tissues internalized lipoprotein-derived cholesterol through the coated-pit pathway, while cholesterol derived from other sources, namely the endogenous synthesis of cholesterol and selective uptake of cholesteryl ester carried in HDL through the scavenger receptor-class B, type I (SR-BI) pathway, did not contribute to the accumulation of cholesterol in the NPC1 mouse [Xie et al., 1999a,b, 2000b]. Importantly, these studies demonstrated that all tissues in the NPC1 mouse had an increased rate of cholesterol synthesis that fully compensated for the decreased availability of lipoprotein-derived cholesterol that became sequestered within late endosomes/lysosomes, thereby causing an increased flow of cholesterol from extrahepatic tissues to the liver by reverse cholesterol transport [Xie et al., 1999b, 2000b]. Consistent with this result, an independent study confirmed that the amount of biliary cholesterol secreted from NPC1 mice was actually increased [Amigo et al., 2002]. Moreover, it was determined that the liver, shown to have the highest uptake of lipoprotein-derived cholesterol and synthesis of cholesterol when compared to other tissues in the mouse, expressed the highest relative amounts of NPC1 mRNA and protein, although it was shown that the relative amount of NPC1 mRNA and protein was not regulated by the amount of cholesterol flowing through cells in the mouse [Garver et al., 2005].

It is well known that the liver serves a central role in maintaining whole-body cholesterol metabolism [Dietschy et al., 1993; Osono et al., 1995, 1996; Turley et al., 1995]. Studies have indicated that approximately one-half of NPC1 patients may suffer from liver disease and that NPC1 disease may be the most common metabolic disorder responsible for neonatal cholestasis [Kelly et al., 1993; Yerushalmi et al., 2002]. This being the case, the pathophysiology associated with NPC1 liver disease and aspects of lipoprotein metabolism have only recently been investigated using the NPC1 mouse [Amigo et al., 2002; Beltroy et al., 2005; Erickson et al., 2005]. To further investigate liver disease and lipoprotein metabolism resulting from partial and complete loss of NPC1 protein function, the present study was performed using livers and serum from normal (NPC1$^{+/+}$), heterozygous (NPC1$^{+/-}$), and homozygous affected (NPC1$^{-/-}$) mice. The study was performed using fasted male mice at 35 days of age before the development of weight loss and neurological symptoms. This age of mouse represented an early to intermediate time period before the premature death of NPC1$^{-/-}$ mice that occurs between 70 and 91 days of age.

MATERIALS AND METHODS

Chemicals and Reagents

Cholesterol, cholesteryl ester, triacylglycerol, and free fatty acid standards for identification of

lipids after separation using thin-layer chromatography were purchased from Sigma Chemical Company (St. Louis, MO). Assay kits to determine the concentration of serum albumin, bilirubin, alanine aminotransferase (ALT), and aspartate aminotransferase (AST), in addition to normal control serum (Data-Trol N) and abnormal control serum (Data-Trol A), were purchased from Thermo Electron Corporation (Lewisville, CO). Assay kits to determine the concentration of liver triacylglycerol using the glycerol kinase-glycerol phosphate oxidase (GK-GPO) method and free fatty acids using the acyl-CoA synthetase-acyl-CoA oxidase (ACS-ACOD) method were purchased from Wako Chemicals (Richmond, VA). Complete protease inhibitor cocktail tablets were purchased from Boehringer Mannheim (Indianapolis, IN). To extract RNA and then generate cDNA, the RNeasy Mini Kit and RNase-free DNase kit were purchased from Qiagen (Valencia, CA). To perform real-time RT-PCR, the TaqMan Gene Expression Assay and TaqMan PCR Master Mix were purchased from Applied Biosystems (Foster City, CA). The kaleidoscope prestained molecular weight protein standards for sodium dodecylsulphate–polyacrylamide gel electrophoresis (SDS–PAGE) were purchased from BioRad Laboratories (Hercules, CA). The high molecular weight native protein standards for nondenaturing–polyacrylamide gel electrophoresis (ND–PAGE) were purchased from Amersham Biosciences (Buckinghamshire, UK). The ABCA1, LDLR, SR-BI, and SR-BII antibodies were purchased from Novus Biologicals (Littleton, CO). The LRP (heavy chain) antibody was purchased from Calbiochem (La Jolla, CA). The β-actin antibody was purchased from Sigma Chemical Company (St. Louis, MO). The nucleophorin p62 antibody was purchased from BD Biosciences (San Diego, CA). Peroxidase-conjugated goat secondary antibodies were purchased from Jackson Immunoresearch Laboratories (West Grove, PA). The West Pico SuperSignal Substrate for Western blotting and bicinchoninic acid (BCA) protein assay kits was purchased from Pierce Chemical Company (Rockford, IL). The BioMax MR film was purchased from Eastman Kodak (New Haven, CT).

BALB/cJ NPC1 Mice

A breeding pair of BALB/cJ heterozygous NPC1 (BALB/cJ $Npc1^{NIH}$) mice was obtained from The Jackson Laboratory (Bar Harbor, ME). The mice were maintained at the University of Arizona Animal Care Facility and managed by the Genetically Modified Mouse Shared Service in the Department of Pediatrics at the University of Arizona. The mice were fed a low-cholesterol 0.2% (wt/wt), low-fat 6% (wt/wt) basal mouse diet (NIH-31, Harlan Teklad, Madison, WI), and water ad libitum in rooms with alternating 12-h periods of light and dark. These mice were bred to produce normal ($NPC1^{+/+}$), heterozygous ($NPC1^{+/-}$), and homozygous affected ($NPC1^{-/-}$) mice. The present study was performed using male mice that were 35 days of age and fasted overnight (16–18 h).

Genotype Analysis of BALB/cJ NPC1 Mice

At the time of weaning (21 days), the BALB/cJ NPC1 mice were genetically identified using DNA prepared from tail-tips. Polymerase chain reactions (PCRs) were performed to identify genotypes residing at the *NPC1* locus using primer pairs as previously described [Loftus et al., 1997]. In brief, PCR amplification buffer (10 mM Tris pH 8.3, 50 mM KCl, 2.5 mM MgCl, 200 mM dNTPs, 1.25 U Taq DNA polymerase, and 1.0 mM of each primer) was used with 20–40 ng of tail-tip DNA added at 85°C, followed by amplification that was performed for 35 cycles of 30 s at 95°C, 30 s at 61°C, and 1 min at 72°C, with a 10 min 72°C terminal extension. The PCR products were separated using a 1.2% agarose gel and visualized with UV light.

Lipid Mass Analysis of Mouse Livers

Mouse livers were removed and homogenized in ice-cold hypotonic homogenization buffer (10 mM sodium phosphate pH 7.4 containing a complete protease inhibitor cocktail) using a motor-driven Teflon and glass homogenizer. A fraction of the tissue homogenate was removed and diluted into 10 parts hexane/isopropanol (3:2, v/v) for 1 h to extract total lipids. The extraction solution was centrifuged to recover a protein pellet and supernatant. The supernatant was dried with nitrogen gas, resuspended into chloroform, and then applied onto a thin-layer chromatography plate developed using hexane/diethyl ether/glacial acetic acid (80:20:1, v/v/v). Cholesterol, cholesteryl ester, triacylglycerol, and free fatty acid were identified by comigration with corresponding standards by staining with iodine vapor. The lipids were scraped from the plate and extracted with

hexane/water (3:1, v/v). After the hexane phase was dried with nitrogen gas, the mass of cholesterol and cholesteryl ester was determined using the cholesterol oxidase method [Heider and Boyett, 1978]. The mass of triacylglycerol and free fatty acid were determined using the glycerol kinase-glycerol phosphate oxidase (GK-GPO) and acyl-CoA synthetase-acyl-CoA oxidase (ACS-ACOD) methods, respectively. The resulting mass of each lipid was normalized to the corresponding protein that was precipitated with organic solvent and determined using the BCA protein assay method.

Lipoprotein Profile Analysis of Mouse Serum

The concentration and distribution of phospholipid and cholesterol associated with HDL, LDL, and VLDL were determined using the lipoprotein autoprofiler method [Chung et al., 1980, 1981]. In brief, an equivalent amount of pooled serum from five $NPC1^{+/+}$, $NPC1^{+/-}$, and $NPC1^{-/-}$ mice was used to perform this study. This method used (i) a short (150 min) single-spin density gradient ultracentrifuge separation of the major lipoprotein fractions in serum with a swing-out rotor (Beckman SW 50.1), (ii) a continuous-flow online-mixing of effluents that were removed from bottom of the density gradient tubes with subsequent enzymatic analysis for phospholipids (Wako Diagnostics) and cholesterol (Sigma Chemical Company), and (iii) online-measurement of absorbance with a computerized calculation to determine the resulting concentration of phospholipid and cholesterol associated with the HDL, LDL, and VLDL density fractions.

Mouse Liver Homogenization and Enrichment of Cellular Fractions

Mouse livers were homogenized in ice-cold hypotonic homogenization buffer (10 mM sodium phosphate pH 7.4 containing a complete protease inhibitor cocktail) using a motor-driven Teflon and glass homogenizer. Slow-speed centrifugation (1,000*g*, 10 min) was performed to enrich the nuclei fraction, followed by high-speed ultracentrifugation (100,000*g*, 1 h) of the post-nuclear supernatant to enrich the total membrane fraction. The proteins associated with the nuclei and total membrane fractions were solubilized with ice-cold solubilization buffer (10 mM sodium phosphate pH 7.4, 150 mM NaCl, 1.0% Triton X-100, and 10 mM SDS containing a complete protease inhibitor cocktail). In preparation for immunoblot analysis, the concentration of protein in the nuclei and total membrane fractions were determined using the BCA protein assay method.

Immunoblot Analysis of Mouse Serum and Cellular Fractions

Protein samples from serum and cellular factions were separated using SDS–PAGE under reduced conditions [Laemmli, 1970]. To determine the relative amount and migration of proteins using SDS–PAGE, kaleidoscope prestained protein standards of known molecular weight (myosin, 210 kDa; beta-galactosidase, 123 kDa; bovine serum albumin, 83 kDa; carbonic anhydrase, 34 kDa; soybean trypsin inhibitor, 28 kDa; and lysozyme, 20 kDa) were used. To determine the particle size of lipoproteins using ND–PAGE, high molecular weight native protein standards of known hydrated Stokes diameter (thyroglobulin, 17.0 nm; ferritin, 12.20 nm; catalase, 10.4 nm; lactate dehydrogenase, 8.2 nm; and albumin, 7.1 nm) were used. After separation using either SDS–PAGE or ND–PAGE, proteins were transferred to a nitrocellulose membrane for immunoblot analysis. In brief, blocking buffer (10 mM sodium phosphate pH 7.4, 150 mM NaCl, 0.05% Tween 20, and 4% non-fat dry milk) was used for 2 h to block nonspecific sites on the nitrocellulose membrane. Immunoblots were incubated overnight at 4°C with primary antibody, followed then by rinsing (3×10 min) to remove residual primary antibody. The peroxidase-conjugated goat secondary antibodies were incubated at room temperature for 1 h, followed then by rinsing (3×10 min) to remove residual secondary antibody. Finally, enhanced chemiluminescence (ECL) was performed with the resulting autoradiograms being obtained on film. In certain studies, the amounts of target protein (ABCA1, p-SREBP-1, n-SREBP-1, p-SREBP-2, and n-SREBP-2) and endogenous control protein (β-actin or nucleophorin p62) were quantified for normalization within the linear range of film using a BioRad Model GS-700 Imaging Densitometer. To determine the size of lipoproteins using ND-PAGE, the distance of migration for respective lipoprotein bands, identified using antibodies against specific apolipoproteins, were measured and assigned an R_f value (R_f value being defined as the distance of migration for respective bands relative to the

distance of migration for the high molecular weight globular protein standards with known hydrated Stokes diameter). A calibration curve with R_f values versus the Stokes diameter for these protein standards was used to calculate the Stokes diameter for the unknown lipoproteins.

Real-Time RT-PCR Analysis of Mouse Liver

The amounts of ABCA1, SREBP-1, and SREBP-2 mRNA were determined using real-time reverse transcription-polymerase chain reaction (RT-PCR) analysis. In brief, total RNA was extracted from mouse livers using the RNeasy Mini Kit, followed by treatment of the RNA with RNase-free DNase to remove contaminating DNA. The concentration of RNA was determined by measuring the absorbance at 260 nm using a spectrophotometer. Reverse transcription was performed using a 40 μl solution that contained 1.0 μg total RNA, 2.5 μM random hexamers, 4.0 mM dNTPs, 15 mM $MgCl_2$, 50 U reverse transcriptase, and 100 U RNA inhibitor to produce complementary DNA (cDNA). Finally, real-time RT-PCR was performed using the cDNA, a TaqMan Gene Expression Assay that contained a 20× mixture of unlabeled PCR primers and Taqman MGB probe (FAM dye-labeled), along with the Taqman Universal PCR Master Mix. This assay was designed for the detection and quantification of specific genetic sequences in RNA samples converted to cDNA using an ABI-PRISM Sequence Detection System (Applied Biosystems). The relative amounts of ABCA1, SREBP-1, and SREBP-2 mRNA were normalized to endogenous 18S rRNA and reported as fold change.

Calculations and Statistical Analysis

For all experiments, quantitative data are represented as the mean ± standard deviation (SD) of three or five normal ($NPC1^{+/+}$), heterozygous ($NPC1^{+/-}$), and homozygous ($NPC1^{-/-}$) mice within each group. Significant differences ($P \leq 0.05$) between groups of data were determined using the two-tailed Student's *t*-test assuming equal variance.

RESULTS

Mouse Body Weight, Liver Weight, and Percent Liver Weight

This study was performed to determine the body weight, liver weight, and percent liver weight of $NPC1^{+/+}$, $NPC1^{+/-}$, and $NPC1^{-/-}$ mice at 35 days of age (Fig. 1). The results indicated no significant difference in the average body weight for $NPC1^{+/+}$, $NPC1^{+/-}$, and

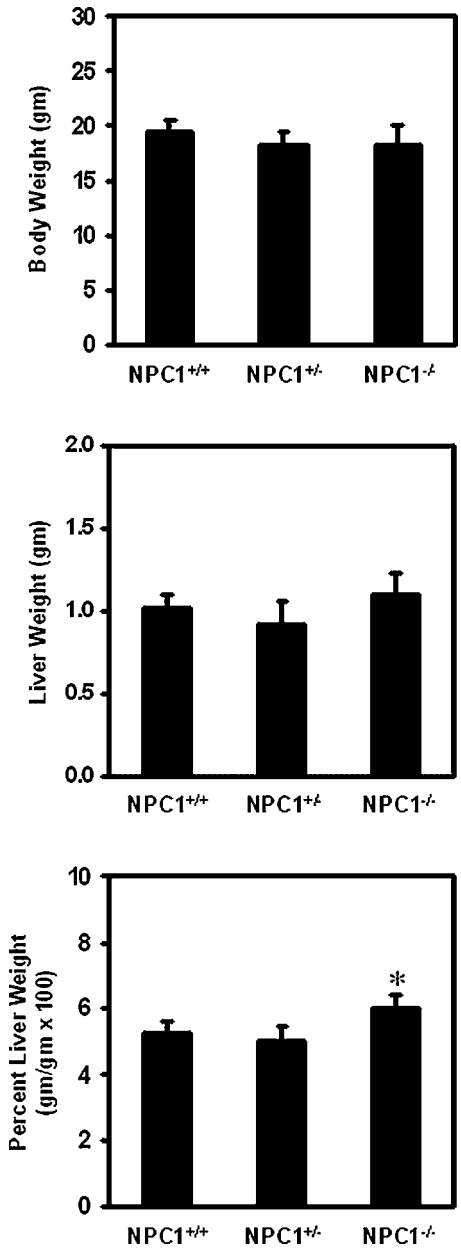

Fig. 1. Mouse body weight, liver weight, and percent liver weight. The mouse body weight, liver weight, and percent liver weight were obtained for normal ($NPC1^{+/+}$), heterozygous ($NPC1^{+/-}$), and homozygous affected ($NPC1^{-/-}$) mice at 35 days of age to determine the presence of hepatomegaly. A graphical representation of the mouse body weight (**top graph**), liver weight (**middle graph**), and percent liver weight (**bottom graph**) are shown. The values represent the mean ± SD obtained from five mice of each genotype. The asterisk represents a statistically significant difference ($P \leq 0.05$).

$NPC1^{-/-}$ mice, although the average body weight for $NPC1^{+/-}$ mice (18.3 g) and $NPC1^{-/-}$ mice (18.3 g) were both slightly decreased compared to the average body weight for $NPC1^{+/+}$ mice (19.4 g). Moreover, there was no significant difference in the average liver weight for $NPC1^{+/+}$, $NPC1^{+/-}$, and $NPC1^{-/-}$ mice, although the average liver weight for $NPC1^{+/-}$ mice (0.9 g) was slightly decreased and the average liver weight for $NPC1^{-/-}$ mice (1.1 g) was slightly increased compared to the average liver weight for $NPC1^{+/+}$ mice (1.0 g). With respect to the average percent liver weight of these mice, there was a significant increase in the average percent liver weight for $NPC1^{-/-}$ mice (6.0%) compared to the average percent liver weight for $NPC1^{+/+}$ mice (5.3%) and $NPC1^{+/-}$ mice (5.0%).

Liver Cell Damage Analysis of Mouse Livers

This study was performed to determine the amount of liver cell damage in $NPC1^{+/+}$, $NPC1^{+/-}$, and $NPC1^{-/-}$ mice at 35 days of age by measuring the concentration of albumin, bilirubin, ALT, and AST in mouse serum (Fig. 2). The results indicated there was no significant difference in the concentration of albumin (top left graph) and bilirubin (top right graph) in $NPC1^{+/+}$, $NPC1^{+/-}$, and $NPC1^{-/-}$ serum, and that the absolute concentration of albumin and bilirubin in serum was within normal limits for albumin (3.5–4.8 g/dl) and bilirubin (0.0–1.5 mg/dl). These results suggested an absence of obstructive cholestasis in $NPC1^{+/-}$ and $NPC1^{-/-}$ mice at 35 days of age, consistent with the transient nature of neonatal jaundice that sometimes occurs in patients with NPC1 disease. In contrast, the results also indicated a slight but significant increase in the concentration of ALT (bottom left graph) and AST (bottom right graph) in $NPC1^{-/-}$ serum compared to $NPC1^{+/+}$ and $NPC1^{+/-}$ serum, and that the absolute concentration of ALT and AST measured in $NPC1^{+/+}$ and $NPC1^{+/-}$ serum was within the normal limits for ALT (10–35 U/l) and AST (5–34 U/l).

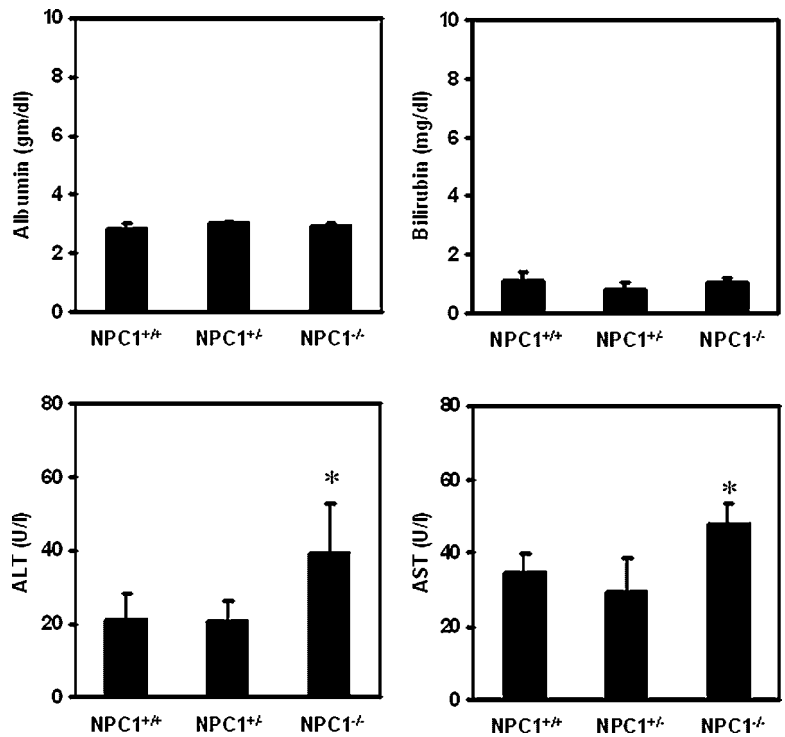

Fig. 2. Liver cell damage analysis of mouse livers. A similar amount of serum was obtained from normal ($NPC1^{+/+}$), heterozygous ($NPC1^{+/-}$), and homozygous affected ($NPC1^{-/-}$) mice at 35 days of age to determine the amount of liver cell damage. A graphical representation for the concentration of albumin (**upper left graph**), bilirubin (**upper right graph**), ALT (**lower left graph**), and AST (**lower right graph**) in serum was determined using standardized colorimetric and ultraviolet analytical kits. The accuracy and precision of these analyses were monitored using normal (Data-Trol N) and abnormal (Data-Trol A) control serum. The values represent the mean $\pm$ SD obtained from five mice of each genotype. The asterisks represent a statistically significant difference ($P \leq 0.05$).

Lipid Mass Analysis of Mouse Livers

This study was performed to determine the mass of cholesterol, cholesteryl ester, triacylglycerol, and free fatty acid in NPC1$^{+/+}$, NPC1$^{+/-}$, and NPC1$^{-/-}$ mouse livers at 35 days of age (Fig. 3). As expected, the mass of cholesterol in NPC1$^{-/-}$ mouse livers was significantly increased (approximately four-fold) compared to the mass of cholesterol in NPC1$^{+/+}$ and NPC1$^{+/-}$ mouse livers (top left graph). With respect to the mass of cholesteryl ester, the results indicated no significant difference in NPC1$^{+/+}$, NPC1$^{+/-}$, and NPC1$^{-/-}$ mouse livers (top right graph). However, unexpectedly the results indicated that the mass of triacylglycerol in NPC1$^{+/-}$ mouse livers was significantly increased (approximately 1.4-fold) compared to the mass of triacylglycerol in NPC1$^{+/+}$ and NPC1$^{-/-}$ mouse livers (bottom left graph). Finally, there was no significant difference in the mass of free fatty acid in NPC1$^{+/+}$, NPC1$^{+/-}$, and NPC1$^{-/-}$ mouse livers (bottom right graph).

Apolipoprotein and Lipoprotein Analysis of Mouse Serum

This study was performed to determine the relative amount of apoA-I, apoB-48, apoB-100, and apoE, in addition to the relative size of apoA-I, apoB-48, apoB-100, and apoE containing lipoproteins in pooled serum from NPC1$^{+/+}$, NPC1$^{+/-}$, and NPC1$^{-/-}$ mice at 35 days of age (Fig. 4). The results using SDS–PAGE indicated that the relative amount of apoA-I in pooled serum was similar in NPC1$^{+/+}$, NPC1$^{+/-}$, and NPC1$^{-/-}$ mice (upper left image). However, the results using ND-PAGE also indicated that the relative distribution of apoA-I between different lipoprotein classes was different in NPC1$^{-/-}$ mice, compared to NPC1$^{+/+}$ and NPC1$^{+/-}$ mice (upper right image). Specifically, while the serum from NPC1$^{+/+}$ and NPC1$^{+/-}$

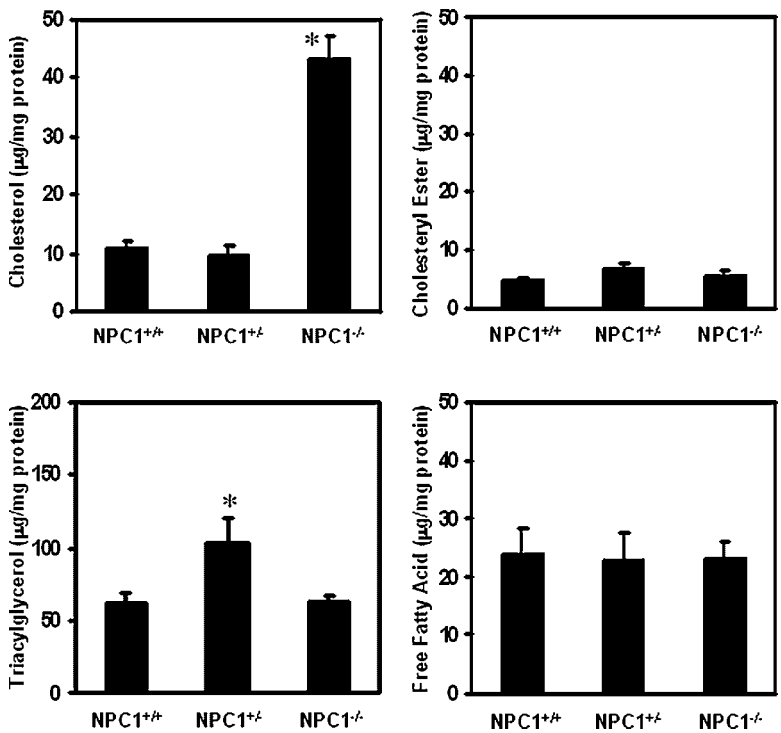

Fig. 3. Lipid mass analysis of mouse livers. Similar sections of mouse liver were obtained from normal (NPC1$^{+/+}$), heterozygous (NPC1$^{+/-}$), and homozygous affected (NPC1$^{-/-}$) mice at 35 days of age to perform lipid mass analysis. The lipids were extracted, separated using thin-layer chromatography, and removed from the plate for lipid mass analysis. The mass of cholesterol and cholesteryl ester were determined using the cholesterol oxidase method, while the mass of triacylglycerol and free fatty acid were determined using the glycerol kinase-glycerol phosphate oxidase (GK-GPO) and acyl-CoA synthetase-acyl-CoA oxidase (ACS-ACOD) methods, respectively. The mass of cholesterol (**upper left graph**), cholesteryl ester (**upper right graph**), triacylglycerol (**lower left graph**), and free fatty acid (**lower right graph**) were normalized to the corresponding protein that was precipitated during extraction with organic solvent. The values represent the mean ± SD obtained from five mice of each genotype. The asterisks represent a statistically significant difference ($P \leq 0.05$).

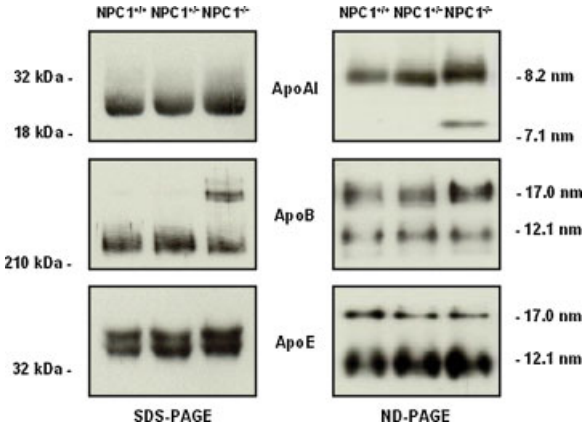

Fig. 4. Apolipoprotein and lipoprotein analysis of mouse serum. An equivalent amount of pooled serum from normal ($NPC1^{+/+}$), heterozygous ($NPC1^{+/-}$), and homozygous affected ($NPC1^{-/-}$) mice at 35 days of age was used to determine the relative amount of apoA-I, apoB-48, apoB-100, and apoE, in addition to the size of apoA-I, apoB-48, apoB-100, and apoE containing lipoproteins. These studies were performed by separating 1.0 µl of pooled serum from five mice represented within each genotype using SDS–PAGE and ND-PAGE, followed by transfer of the separated proteins to a nitrocellulose membrane for immunoblot analysis. Protein bands were visualized using ECL and the resulting autoradiograms were obtained on film. For SDS–PAGE, prestained molecular weight protein standards were used to determine the migration of respective apolipoproteins (**left images**). For ND-PAGE, high molecular weight native protein standards with known hydrated Stokes diameter were used to determine the migration and calculate the Stokes diameter of the respective lipoproteins (**right images**).

mice contained a major apoA-I lipoprotein with a diameter of 8.1 nm, the serum from $NPC1^{-/-}$ mice had a major apoA-I lipoprotein with a diameter of 8.2 nm. Both of these major apoA-I lipoproteins were within the 8.0–8.4 nm diameter range that would allow these particles to be classified as either HDL_{3a} or HDL_{3b}, consistent with HDL_3 accounting for over 90% of all HDL that is present in mouse serum [Camus et al., 1983]. Since HDL_{3a} is known to represent the larger apoA-I lipoprotein, the results suggest that serum from $NPC1^{-/-}$ mice contained relatively more HDL_{3a}, while serum from $NPC1^{+/+}$ and $NPC1^{+/-}$ mice contained relatively more HDL_{3b}. In addition, the serum from $NPC1^{-/-}$ mice also contained a minor apoA-I lipoprotein with a diameter of 7.6 nm that was not present in serum from $NPC1^{+/+}$ and $NPC1^{+/-}$ mice. It is suspected that this apoA-I lipoprotein with a diameter of 7.6 nm represents HDL_{3c} based upon its smaller diameter. With respect to the amount of apoB in mouse serum, previous studies have determined that the relative amount of apoB-48 is considerably more abundant than apoB-100 [Li et al., 1996]. Consistent with this result, the present study using SDS–PAGE indicated that apoB-48 was the major form of apoB in $NPC1^{+/+}$, $NPC1^{+/-}$, and $NPC1^{-/-}$ mouse serum, and that these mice had relatively similar amounts of apoB-48 (middle left image). However, it was also apparent that while $NPC1^{+/+}$ and $NPC1^{+/-}$ mouse serum contained only apoB-48, the $NPC1^{-/-}$ mouse serum also contained apoB-100 (middle left image). Further investigation of these apoB lipoproteins obtained using ND-PAGE indicated that $NPC1^{+/+}$, $NPC1^{+/-}$, and $NPC1^{-/-}$ mouse serum had a similar distribution of apoB among two classes of lipoproteins (middle right images), where the major class of apoB lipoprotein had a diameter of 17.3 nm and the minor class of apoB lipoprotein had a diameter of 12.0 nm. Finally, the results also indicated that $NPC1^{+/+}$, $NPC1^{+/-}$, and $NPC1^{-/-}$ mouse serum contained similar amounts of apoE, represented by a doublet migrating at 35–38 kDa using SDS–PAGE (bottom left image). These results were confirmed with a similar amount of apoE that was distributed between two classes of lipoproteins described above using ND-PAGE (bottom right image). However, in contrast to apoB that was found to be primarily associated with the lipoprotein having a diameter of 17.3 nm, apoE was primarily associated with the lipoprotein having a diameter of 12.0 nm. Although these results are consistent with previous studies demonstrating that apoB and apoE are commonly associated with the same lipoproteins, the rather small diameter of the 12.0 nm lipoprotein excludes it from representing LDL. Instead, it is suspected that this particle may represent either a large form of HDL (HDL_1) that is known to be devoid of apoA-I but enriched with apoE, or an unusual form of HDL that contains apoB-48 and apoE, recently shown to be assembled and secreted by the intestine while only in the fasted state [De Silva et al., 1994; Guo et al., 2005]. In any event, together these results indicate only minor alterations in the relative amount and distribution of apolipoproteins and lipoproteins in serum from these mice.

Lipoprotein Profile Analysis of Mouse Serum

To further characterize the composition of lipoproteins in mouse serum, the concentration and distribution of phospholipid and cholesterol

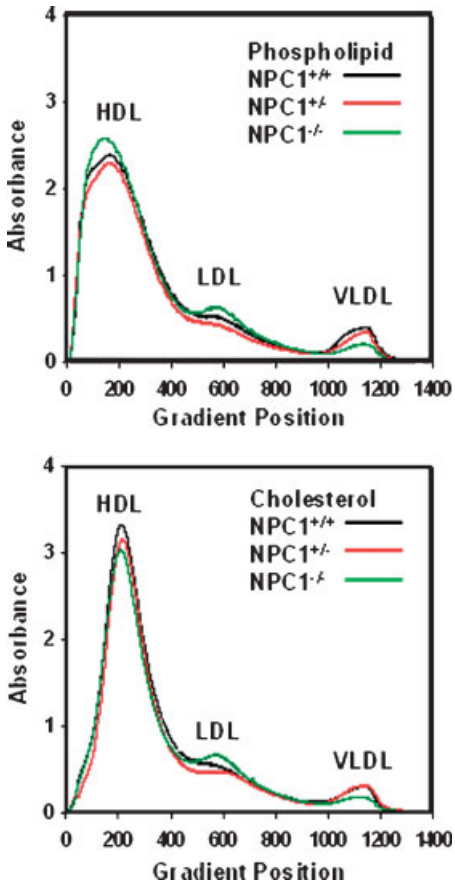

Fig. 5. Lipoprotein profile analysis of mouse serum. An equivalent amount of pooled serum from normal ($NPC1^{+/+}$), heterozygous ($NPC1^{+/-}$), and homozygous affected ($NPC1^{-/-}$) mice at 35 days of age was used to determine the concentration and distribution of phospholipid and cholesterol associated with high density lipoprotein (HDL), low density lipoprotein (LDL), and very low density lipoprotein (VLDL). These studies were performed by separating 100 μl of pooled serum from five $NPC1^{+/+}$ mice (black line), five $NPC1^{+/-}$ mice (red line), and five $NPC1^{-/-}$ mice (green line) using the lipoprotein autoprofiler method to determine the concentration and distribution of phospholipid (**top graph**) and cholesterol (**bottom graph**) associated with the HDL, LDL, and VLDL fractions.

in lipoproteins from $NPC1^{+/+}$, $NPC1^{+/-}$, and $NPC1^{-/-}$ mouse serum at 35 days of age was determined (Fig. 5 and Table I). The results indicted a similar concentration of total phospholipid in $NPC1^{+/+}$ (169.01 mg/dl) and $NPC1^{-/-}$ (169.59 mg/dl) mouse serum, with a slightly decreased concentration of total phospholipid in $NPC1^{+/-}$ (154.81 mg/dl) mouse serum. The results also indicated a similar concentration of HDL phospholipid in $NPC1^{+/+}$ (133.44 mg/dl) and $NPC1^{-/-}$ (134.25 mg/dl) mouse serum, with a slightly decreased concentration of HDL phospholipid in $NPC1^{+/-}$ (124.17 mg/dl) mouse serum. However, there was an equivalent percentage of phospholipid associated with HDL in $NPC1^{+/+}$ (79%), $NPC1^{+/-}$ (80%), and $NPC1^{-/-}$ (79%) mouse serum. In contrast, although the percentage of phospholipid associated with LDL and VLDL in $NPC1^{+/+}$ (14% and 7%, respectively) and $NPC1^{+/-}$ (13% and 7%, respectively) mouse serum were similar, the percentage of phospholipid associated with LDL and VLDL in $NPC1^{-/-}$ (18% and 3%, respectively) mouse serum was altered, with $NPC1^{-/-}$ mouse serum having relatively more phospholipid associated with LDL than VLDL. With respect to the concentration and distribution of cholesterol in mouse serum, the results indicted that compared to the concentration of total cholesterol in $NPC1^{+/+}$ (122.10 mg/dl) mouse serum, the concentration of total cholesterol in $NPC1^{+/-}$ (109.69 mg/dl) and $NPC1^{-/-}$ (112.28 mg/dl) mouse serum was slightly decreased. The results also indicated that compared to the concentration of HDL cholesterol in $NPC1^{+/+}$ (94.03 mg/dl) mouse serum, the concentration of HDL cholesterol in $NPC1^{+/-}$ (84.35 mg/dl) and $NPC1^{-/-}$ (85.61 mg/dl) mouse serum was also

TABLE I. Phospholipid and Cholesterol Composition of HDL, LDL, and VLDL in $NPC1^{+/+}$, $NPC1^{+/-}$, and $NPC1^{-/-}$ Mouse Serum

Genotype	Total-PL (mg/dl)	HDL-PL (mg/dl)	LDL-PL (mg/dl)	VLDL-PL (mg/dl)
$NPC1^{+/+}$	169.01	133.44 (79%)	23.32 (14%)	12.25 (7%)
$NPC1^{+/-}$	154.81	124.17 (80%)	20.32 (13%)	10.32 (7%)
$NPC1^{-/-}$	169.57	134.25 (79%)	29.60 (18%)	5.71 (3%)
Genotype	Total-C (mg/dl)	HDL-C (mg/dl)	LDL-C (mg/dl)	VLDL-C (mg/dl)
$NPC1^{+/+}$	122.10	94.03 (77%)	21.09 (17%)	6.98 (6%)
$NPC1^{+/-}$	109.69	84.35 (77%)	18.71 (17%)	6.63 (6%)
$NPC1^{-/-}$	112.28	85.61 (76%)	22.81 (20%)	3.86 (3%)

The concentration and distribution of phospholipid and cholesterol associated with high density lipoprotein (HDL), low density lipoprotein (LDL), and very low density lipoprotein (VLDL) were determined using the lipoprotein autoprofiler method. Density gradient ultracentrifugation was performed to separate the major lipoprotein fractions, followed by continuous-flow online-mixing of effluents that were removed from the bottom of density gradient tubes and enzymatic analysis of phospholipid (PL) and cholesterol (C). A computerized calculation for the concentration of phospholipid and cholesterol associated with the HDL, LDL, and VLDL density fractions was determined using equivalent amounts of pooled serum from five mice of each genotype.

slightly decreased. In order to verify whether there was a significant decrease in the concentration of total cholesterol in $NPC1^{+/-}$ and $NPC1^{-/-}$ mouse serum, an independent study was conducted using serum from a different set of $NPC1^{+/+}$, $NPC1^{+/-}$, and $NPC1^{-/-}$ mice. The results indicated that although the average concentration of total cholesterol was again slightly decreased in $NPC1^{+/-}$ and $NPC1^{-/-}$ mouse serum, the differences were not statistically significant (data not shown). Moreover, as described above for the percentage of phospholipid associated with HDL present in mouse serum, there was an equivalent percentage of cholesterol associated with HDL in $NPC1^{+/+}$ (77%), $NPC1^{+/-}$ (77%), and $NPC1^{-/-}$ (76%) mouse serum. Finally, the percentage of cholesterol associated with LDL and VLDL in $NPC1^{+/+}$ (17% and 6%, respectively) and $NPC1^{+/-}$ (17% and 6%, respectively) mouse serum were similar, while the percentage of cholesterol associated with LDL and VLDL in $NPC1^{-/-}$ mice (20% and 3%, respectively) mouse serum was altered, with $NPC1^{-/-}$ mouse serum having relatively more cholesterol associated with LDL than VLDL.

Relative Amounts of ABCA1 mRNA and Protein in Mouse Livers

The present study was performed to determine the relative amounts of ABCA1 mRNA and protein in $NPC1^{+/+}$, $NPC1^{+/-}$, and $NPC1^{-/-}$ mouse livers at 35 days of age (Fig. 6). The results obtained using real-time RT-PCR indicated no significant difference in the relative amounts of ABCA1 mRNA in $NPC1^{+/+}$, $NPC1^{+/-}$, and $NPC1^{-/-}$ mouse livers. Moreover, the results obtained using immunoblot analysis also indicated no significant difference in the relative amounts of ABCA1 protein in $NPC1^{+/+}$, $NPC1^{+/-}$, and $NPC1^{-/-}$ mouse livers. With respect to additional apolipoprotein and lipoprotein receptors, the results obtained using immunoblot analysis indicated that the relative amounts of LDLR, LRP, scavenger receptor-class B, type I (SR-BI), and scavenger receptor-class B, type II (SR-BII) were similar in $NPC1^{+/+}$, $NPC1^{+/-}$, and $NPC1^{-/-}$ mouse livers (data not shown).

Relative Amounts of SREBP mRNA and Protein in Mouse Livers

The present study was performed to determine the relative amounts of SREBP-1 and SREBP-2 mRNA, in addition to the relative amounts of SREBP-1 and SREBP-2 protein, in $NPC1^{+/+}$, $NPC1^{+/-}$, and $NPC1^{-/-}$ mouse livers at 35 days of age (Fig. 7). The results indicated that for $NPC1^{+/+}$, $NPC1^{+/-}$, and $NPC1^{-/-}$ mouse livers analyzed using real-time

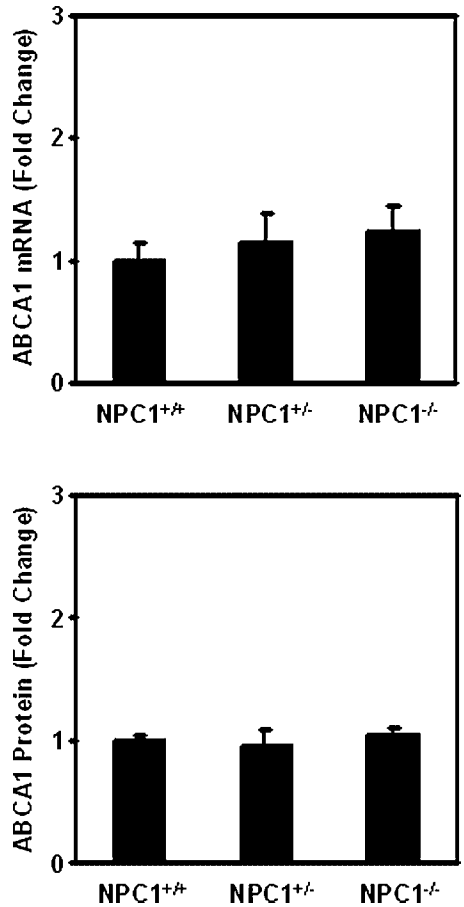

Fig. 6. Relative amounts of ABCA1 mRNA and protein in mouse livers. Similar sections of liver were obtained from normal ($NPC1^{+/+}$), heterozygous ($NPC1^{+/-}$), and homozygous affected ($NPC1^{-/-}$) mice at 35 days of age to determine the relative amounts of ABCA1 mRNA and protein. The relative amounts of ABCA1 mRNA were determined using real-time RT-PCR after normalization to the amounts of corresponding 18S rRNA (internal control). The average amount of ABCA1 mRNA in $NPC1^{+/+}$ mouse livers was assigned an arbitrary value equal to 1.0, with the average amounts of ABCA1 mRNA in $NPC1^{+/-}$ and $NPC1^{-/-}$ mouse livers expressed as fold change relative to the average amount of ABCA1 mRNA in $NPC1^{+/+}$ mouse livers (**top graph**). The relative amounts of ABCA1 protein were determined using immunoblot analysis after normalization to the amounts of corresponding β-actin (internal control). The average amount of ABCA1 protein in $NPC1^{+/+}$ mouse livers was assigned an arbitrary value equal to 1.0, with the average amounts of ABCA1 protein in $NPC1^{+/-}$ and $NPC1^{-/-}$ mouse livers expressed as fold change relative to the average amount of ABCA1 protein in $NPC1^{+/+}$ mouse livers (**bottom graph**). The values represent the mean ± SD obtained from three mice of each genotype.

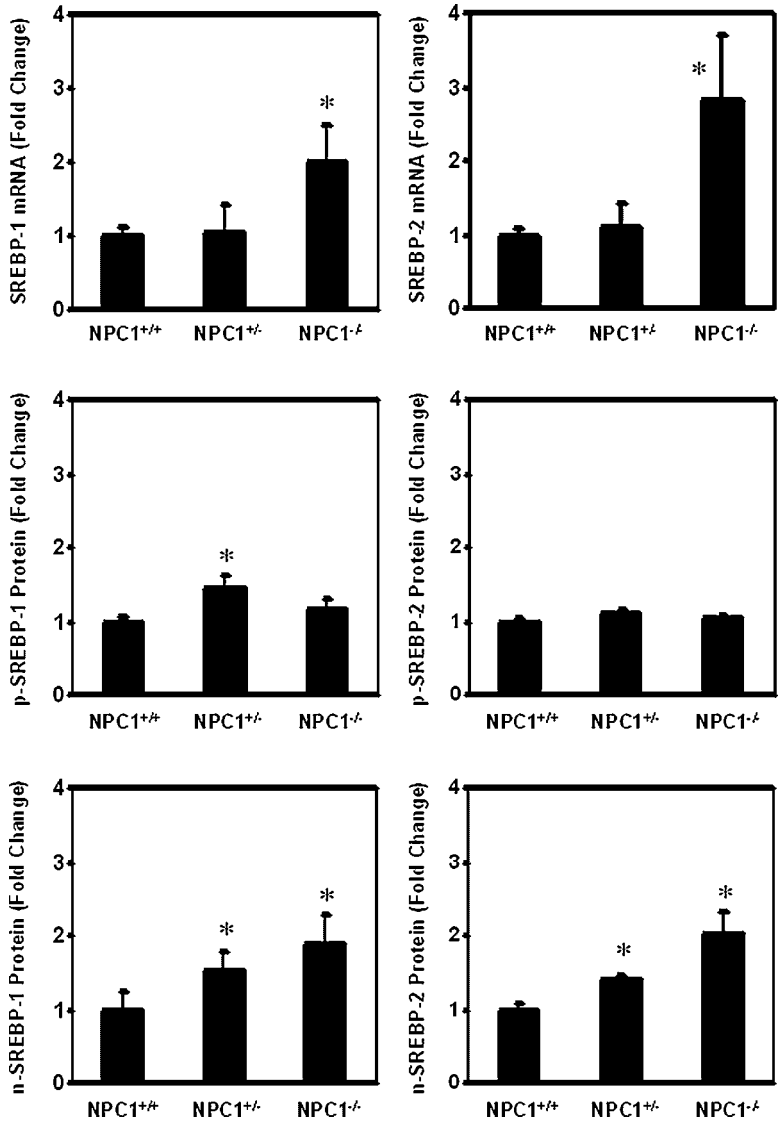

Fig. 7. Relative amounts of SREBP mRNA and protein in mouse livers. Similar sections of liver were obtained from normal ($NPC1^{+/+}$), heterozygous ($NPC1^{+/-}$), and homozygous affected ($NPC1^{-/-}$) mice at 35 days of age to determine the relative amounts of SREBP-1 and SREBP-2 mRNA and protein. The relative amounts of SREBP-1 and SREBP-2 mRNA were determined using real-time RT-PCR after normalization to the amounts of corresponding 18S rRNA (internal control). The average amounts of SREBP-1 and SREBP-2 mRNA in $NPC1^{+/+}$ mouse livers were assigned an arbitrary value equal to 1.0, with the average amounts of SREBP-1 and SREBP-2 mRNA in $NPC1^{+/-}$ and $NPC1^{-/-}$ mouse livers expressed as fold change relative to the average amounts of SREBP-1 and SREBP-1 mRNA in $NPC1^{+/+}$ mouse livers (**top graphs**). The relative amounts of membrane-bound precursor SREBP protein (p-SREBP-1 and p-SREBP-2) were determined using immunoblot analysis after normalization to the amounts of corresponding β-actin (internal control). The average amounts of p-SREBP-1 and p-SREBP-2 in $NPC1^{+/+}$ mouse livers were assigned arbitrary values equal to 1.0, with the average amounts of p-SREBP-1 and p-SREBP-2 in $NPC1^{+/-}$ and $NPC1^{-/-}$ mouse livers expressed as fold change relative to the average amounts of p-SREBP-1 and p-SREBP-2 in $NPC1^{+/+}$ mouse livers (**middle graphs**). The relative amounts of nuclear processed SREBP protein (n-SREBP-1 and n-SREBP-2) were determined using immunoblot analysis after normalization to the amounts of corresponding nucleophorin p62 (internal control). The average amounts of n-SREBP-1 and n-SREBP-2 in $NPC1^{+/+}$ mouse livers were assigned an arbitrary value equal to 1.0, with the average amounts of n-SREBP-1 and n-SREBP-2 in $NPC1^{+/-}$ and $NPC1^{-/-}$ mouse livers expressed as fold change relative to the average amounts of n-SREBP-1 and n-SREBP-2 in $NPC1^{+/+}$ mouse livers (**bottom graphs**). The values represent the mean ± SD obtained from three mice of each genotype. The asterisks represent a statistically significant difference ($P \leq 0.05$).

RT-PCR, the relative amount of SREBP-1 mRNA in $NPC1^{-/-}$ mouse livers was significantly increased (approximately two-fold) compared to the amounts of SREBP-1 mRNA in $NPC1^{+/+}$ and $NPC1^{+/-}$ mouse livers. With respect to the relative amounts of SREBP-1 protein that were measured in $NPC1^{+/+}$, $NPC1^{+/-}$, and $NPC1^{-/-}$ mouse livers using immunoblot analysis, the relative amounts of precursor (p)-SREBP-1 and nuclear (n)-SREBP-1 in $NPC1^{+/-}$ mouse livers were significantly increased (both approximately 1.5-fold) compared to the amounts of p-SREBP-1 and n-SREBP-1 in $NPC1^{+/+}$ mouse livers. Moreover, although there was no significant difference in the relative amounts of p-SREBP-1 in $NPC1^{+/+}$ and $NPC1^{-/-}$ mouse livers, the relative amount of n-SREBP-1 in $NPC1^{-/-}$ mouse livers was significantly increased (approximately two-fold) compared to the amount of n-SREBP-1 in $NPC1^{+/+}$ mouse livers. The results also indicated that for $NPC1^{+/+}$, $NPC1^{+/-}$, and $NPC1^{-/-}$ mouse livers analyzed using real-time RT-PCR, the relative amount of SREBP-2 mRNA in $NPC1^{-/-}$ mouse livers was significantly increased (approximately three-fold) compared to the amounts of SREBP-2 mRNA in $NPC1^{+/+}$ and $NPC1^{+/-}$ mouse livers. With respect to the relative amounts of SREBP-2 protein that were measured in $NPC1^{+/+}$, $NPC1^{+/-}$, and $NPC1^{-/-}$ mouse livers using immunoblot analysis, although there were no significant differences in the relative amounts of p-SREBP-2, the relative amounts of n-SREBP-2 in $NPC1^{+/-}$ and $NPC1^{-/-}$ mouse livers were significantly increased (approximately 1.5- and 2.0-fold, respectively) compared to the amount of n-SREBP-2 in $NPC1^{+/+}$ mouse livers. With respect to additional metabolic nuclear transcription factors, the results obtained using immunoblot analysis indicated that the relative amounts of liver X receptor α (LXRα), peroxisome proliferator-activated receptor-alpha (PPARα), and peroxisome proliferator-activated receptor-gamma (PPARγ), were similar in $NPC1^{+/+}$, $NPC1^{+/-}$, and $NPC1^{-/-}$ mouse livers (data not shown).

DISCUSSION

The present study provides an in depth comparative analysis of liver disease, liver lipid metabolism, apolipoprotein and lipoprotein metabolism, and the expression of specific genes using livers and serum from $NPC1^{+/+}$, $NPC1^{+/-}$, and $NPC1^{-/-}$ mice at 35 days of age before the development of weight loss and neurological symptoms due to NPC1 disease. This particular age of mouse represents an early to intermediate time period before the premature death of $NPC1^{-/-}$ mice that typically occurs between 70 and 91 days of age. In brief, the results indicated (i) the presence of mild hepatomegaly in $NPC1^{-/-}$ mice, (ii) the presence of liver cell damage characterized by significant elevations in the concentration of ALT and AST in $NPC1^{-/-}$ mouse serum, (iii) a significant accumulation of triacylglycerol and cholesterol in $NPC1^{+/-}$ and $NPC1^{-/-}$ mouse livers, respectively, (iv) minor differences in the distribution of apolipoproteins associated with lipoproteins in $NPC1^{-/-}$ mouse serum, (v) minor differences in the concentration and distribution of phospholipid and cholesterol associated with lipoproteins in $NPC1^{+/-}$ and $NPC1^{-/-}$ mouse serum, and (vi) a relative increase in the expression and processing of SREBP-1 and SREBP-2 in $NPC1^{+/-}$ and $NPC1^{-/-}$ mouse livers.

To date, few studies have been conducted on NPC1 liver disease, which is surprising since the first symptoms often diagnosed among individuals with NPC1 disease are abnormalities associated with the liver. Studies suggest that approximately one-half of individuals with NPC1 disease present with liver abnormalities during the first few years of life, although these abnormalities may be transient in nature and last only a few months [Kelly et al., 1993; Yerushalmi et al., 2002]. In general, classic NPC1 liver disease has been characterized by prolonged neonatal jaundice with marked hepatomegaly beginning the first few days of life [Jaeken et al., 1980; Rutledge, 1989; Schiffmann, 1996]. In most instances, a child undiagnosed with NPC1 disease may present with liver disease and be broadly diagnosed as having neonatal hepatitis with obstructive cholestasis, as evidence of having elevated bilirubin and alkaline phosphatase levels, in addition to having elevated ALT and AST enzyme levels [Ivemark et al., 1963; Jaeken et al., 1980; Semeraro et al., 1986]. A liver biopsy from such children has revealed the presence of pleomorphic, enlarged, and vacuolated hepatocytes containing numerous dense and membranous inclusions within the cytoplasm [Ashkenazi et al., 1971; Semeraro et al., 1986].

It has subsequently been shown that approximately 10% of these children with NPC1 disease that present with neonatal cholestasis eventually die of liver failure before the onset of neurological symptoms [Kelly et al., 1993; Yerushalmi et al., 2002].

In light of a recent complimentary study that characterized liver function in $NPC1^{-/-}$ mice between 1 and 75 days of age, the present study was performed at a point in time whereby the level of alkaline phosphatase should have been normalized and the levels of ALT and AST only beginning to increase [Beltroy et al., 2005]. Indeed, in the present study while the concentration of bilirubin in $NPC1^{+/+}$ and $NPC1^{-/-}$ mouse serum were similar at 35 days of age, the concentration of ALT and AST in $NPC1^{-/-}$ mouse serum was elevated approximately 2- and 1.5-fold, respectively. Moreover, consistent with a rapid onset of hepatomegaly in $NPC1^{-/-}$ mice, while the present study indicated a 1% absolute increase in relative liver to body weight that was present at 35 days of age, the previous study indicated a 2% absolute increase in relative liver to body weight that was present at 42 days of age. Hence, the results suggest that hepatomegaly begins to develop in $NPC1^{-/-}$ mice at approximately 35 days of age.

To further investigate the storage of lipid that occurs in NPC1 disease, the relative mass of cholesterol, cholesteryl ester, triacylglycerol, and free fatty acid was determined in $NPC1^{+/+}$, $NPC1^{+/-}$, and $NPC1^{-/-}$ mouse livers. As anticipated, the results clearly indicated a significant increase in the mass of cholesterol in $NPC1^{-/-}$ mouse livers, with both the $NPC1^{+/+}$ and $NPC1^{+/-}$ mouse livers having a similar mass of cholesterol as previously described [Pentchev et al., 1986]. Moreover, consistent with a time-dependent accumulation of lipoprotein-derived cholesterol through the coated-pit pathway, the mass of cholesterol in $NPC1^{-/-}$ mouse livers at 35 days of age (increased approximately four-fold) was lower than the mass of cholesterol in $NPC1^{-/-}$ mouse livers at 42 days of age (increased approximately eight-fold) and at 49 days of age (increased over ten-fold), compared to the mass of cholesterol in $NPC1^{+/+}$ mouse livers measured at the same age [Xie et al., 1999b; Amigo et al., 2002]. With respect to the accumulation of neutral lipids, the results also indicated that while the relative mass of cholesteryl ester was similar in $NPC1^{+/+}$, $NPC1^{+/-}$, and $NPC1^{-/-}$ mouse livers, the mass of triacylglycerol was significantly increased in $NPC1^{+/-}$ mouse livers, compared to both $NPC1^{+/+}$ and $NPC1^{-/-}$ mouse livers. The increased mass of triacylglycerol in $NPC1^{+/-}$ mouse livers was verified using both histochemical analysis by staining tissues with Oil Red O, in addition to performing transmission electron microscopy which revealed an increased number of enlarged lipid bodies present within the perinuclear region of $NPC1^{+/-}$ hepatocytes (data not shown). Although not previously reported, the accumulation of triacylglycerol in $NPC1^{+/-}$ hepatocytes is somewhat similar to that described for nonalcoholic fatty liver disease (NAFLD), which is now believed to represent the most common cause of chronic liver disease [Clark et al., 2002]. Finally, the results also indicated there was no significant difference in the relative mass of free fatty acids in $NPC1^{+/+}$, $NPC1^{+/-}$, and $NPC1^{-/-}$ mouse livers, thereby providing the first in vivo evidence suggesting that the NPC1 protein does not function to facilitate the transport of free fatty acids, consistent with other recent studies performed in vitro using NPC1 human fibroblasts [Passeggio and Liscum, 2005].

It has been well established that the liver serves a primary role in lipoprotein metabolism [Turley and Dietschy, 1988; Dietschy and Turley, 2002]. However, in light of the liver abnormalities associated with NPC1 disease, there have been few detailed studies performed to investigate aspects of lipoprotein metabolism in the NPC1 mouse [Xie et al., 1999a, 2000b; Amigo et al., 2002]. The results in the present study indicated that compared to $NPC1^{+/+}$ mice, both $NPC1^{+/-}$ and $NPC1^{-/-}$ mice had only minor differences associated with aspects of apolipoprotein and lipoprotein metabolism. First, with respect to apoB containing lipoproteins, it was determined that although $NPC1^{+/+}$ and $NPC1^{+/-}$ mice expressed only apoB-48, $NPC1^{-/-}$ mice expressed both apoB-48 and apoB-100. Moreover, although the concentration of phospholipid and cholesterol associated with VLDL was relatively decreased in $NPC1^{-/-}$ mice, the concentration of phospholipid and cholesterol associated with LDL in $NPC1^{-/-}$ mice was proportionally increased. Although speculative, these differences may have resulted from a decreased incorporation of available cholesterol into nascent VLDL particles produced and secreted from $NPC1^{-/-}$ hepatocytes. Second, with respect to apoA-I

lipoproteins, while $NPC1^{+/+}$ and $NPC1^{+/-}$ mice contained only one major apoA-I lipoprotein with a diameter of 8.1 nm, the $NPC1^{-/-}$ mice had a major apoA-I lipoprotein with a diameter of 8.2 nm, in addition to another minor apoA-I lipoprotein with a diameter of 7.6 nm. Although the basis for this particular difference in apoA-I lipoproteins remains undefined, similar results have been reported previously whereby $NPC1^{-/-}$ mice were shown to have slightly enlarged and more heterogeneous HDL particles [Amigo et al., 2002].

The results from the present study determined that the concentration of total and HDL cholesterol were similar in $NPC1^{+/+}$, $NPC1^{+/-}$, $NPC1^{-/-}$ mice at 35 days of age. Interestingly, these results are in direct contrast to other studies that have demonstrated an increased concentration of total and HDL cholesterol in $NPC1^{-/-}$ mice at 42 and 49 days of age [Xie et al., 1999a; Amigo et al., 2002]. In an attempt to investigate this difference, the concentration of total and HDL cholesterol was determined in $NPC1^{+/+}$ and $NPC1^{-/-}$ mice at approximately 45 days of age. As previously reported for these older $NPC1^{+/+}$ and $NPC1^{-/-}$ mice, the results indicated that $NPC1^{-/-}$ mice have an increased concentration of total and HDL cholesterol (data not shown), suggesting that after approximately 35 days of age the concentration of total and HDL cholesterol increases in $NPC1^{-/-}$ mice. Although speculative, a possible explanation for these results may include an overall increased synthesis of peripheral tissue and liver cholesterol in the older $NPC1^{-/-}$ mice to compensate for the continual sequestration of lipoprotein-derived cholesterol in late endosomes/lysosomes, thereby increasing the overall flow of total and HDL cholesterol from tissues back to the liver by reverse cholesterol transport to be secreted as biliary cholesterol, which has been shown to be increased in $NPC1^{-/-}$ mice [Xie et al., 1999a, 2000b; Amigo et al., 2002]. An additional explanation may include the increased loss of myelin-associated cholesterol and the release of sequestrated neuronal cholesterol that is believed to occur in older $NPC1^{-/-}$ mice resulting from neurodegeneration [Xie et al., 2000a; Li et al., 2005]. Finally, although humans and mice with NPC1 disease have been characterized as having an early transient cholestasis, a more chronic cholestatic liver disease referred to as primary biliary cirrhosis (PBC) has been shown to be associated with hypercholesterolemia and an increased concentration of HDL cholesterol, thereby providing another possible explanation for the increased total and HDL cholesterol present in older $NPC1^{-/-}$ mice [O'Kane et al., 1997; Longo et al., 2002].

A number of studies have now determined that ABCA1 functions primarily in the liver to facilitate the lipidation of apoA-I, and that the function of ABCA1 in the liver is directly related to the concentration of HDL cholesterol [Haghpassand et al., 2001; Basso et al., 2003; Tsujita et al., 2005]. In the present study, the relative amount of ABCA1 mRNA and protein was determined to be similar in $NPC1^{+/+}$, $NPC1^{+/-}$, and $NPC1^{-/-}$ mouse livers, consistent with the similar concentration of total and HDL cholesterol that was measured in the serum from these mice. However, as discussed above, the concentration of total and HDL cholesterol increases in mice after approximately 35 days of age, consistent with previous results indicating that the relative amount and function of ABCA1 protein is increased in older $NPC1^{-/-}$ mouse livers [Amigo et al., 2002; Heidenreich and Garver, 2003]. Nonetheless, these particular results that were obtained using $NPC1^{+/+}$, $NPC1^{+/-}$, and $NPC1^{-/-}$ mice are in direct contrast to other studies that were conducted using $NPC1^{+/+}$, $NPC1^{+/-}$, and $NPC1^{-/-}$ human fibroblasts, whereby the $NPC1^{+/-}$ and $NPC1^{-/-}$ human fibroblasts were shown to have a decreased relative amount of ABCA1 mRNA and protein, in addition to a decreased level of apoA-I-mediated lipid efflux [Choi et al., 2003]. As a result of this apparent discrepancy, additional studies are now being conducted using $NPC1^{+/+}$, $NPC1^{+/-}$, and $NPC1^{-/-}$ mouse hepatocytes in an attempt to reconcile differences concerning the relative amount and function of ABCA1 in humans and mice with NPC1 disease.

In comparison to $NPC1^{+/+}$ mouse livers, the present study indicates that $NPC1^{-/-}$ mouse livers at approximately 35 days of age have an increased concentration of cholesterol (approximately four-fold), with a relative deficiency of cholesterol that is accessible to the metabolically active pool of cholesterol at the endoplasmic reticulum, as evidence by an increased relative amount of n-SREBP-1 and n-SREBP-2 (approximately two-fold). Interestingly, although other studies have indicated that $NPC1^{-/-}$ mouse livers at approximately 50 days of age have an even greater concentration of

cholesterol (approximately 20-fold), there was a relative excess of cholesterol that was accessible to the metabolically active pool of cholesterol at the endoplasmic reticulum, as evidence by a decreased relative amount of n-SREBP-1 (approximately two-fold) [Erickson et al., 2000, 2001]. Although speculative, it is therefore proposed that the continued sequestration of lipoprotein-derived cholesterol within late endosomes/lysosomes of NPC1$^{-/-}$ mouse livers may reach a critical limit, after which cholesterol is released in an unregulated manner to other cellular compartments. Consistent with this proposal are studies demonstrating the accumulation of cholesterol and subsequent generation of oxysterol within late endosomes/lysosomes, eventually responsible for causing organelle damage and destabilization [Yuan et al., 1997, 2000]. Importantly, the unregulated release of cholesterol and/or oxysterol from damaged and destabilized late endosomes/lysosomes may provide an explanation for the time-dependent accumulation of cholesterol within mitochondrial membranes of NPC1$^{-/-}$ cells that were grown in culture [Yu et al., 2005; Huang et al., 2006]. The resultant accumulation of cholesterol within mitochondrial membranes may then be responsible for promoting generalized mitochondria dysfunction to adversely affect overall intracellular cholesterol homeostasis and predisposing cells to apoptosis [Beltroy et al., 2005; Li et al., 2005; Huang et al., 2006].

A diagrammatic representation of the proposed consequences for time-dependent accumulation of lipoprotein-derived cholesterol through the coated-pit pathway in NPC1$^{-/-}$ mouse hepatocytes is provided (Fig. 8). In brief, previous studies have determined that tissues from NPC1$^{-/-}$ mice continuously acquire cholesterol from the internalization of sterol carried within certain lipoproteins (chylomicron remnants, VLDL remnants, LDL) and inter-

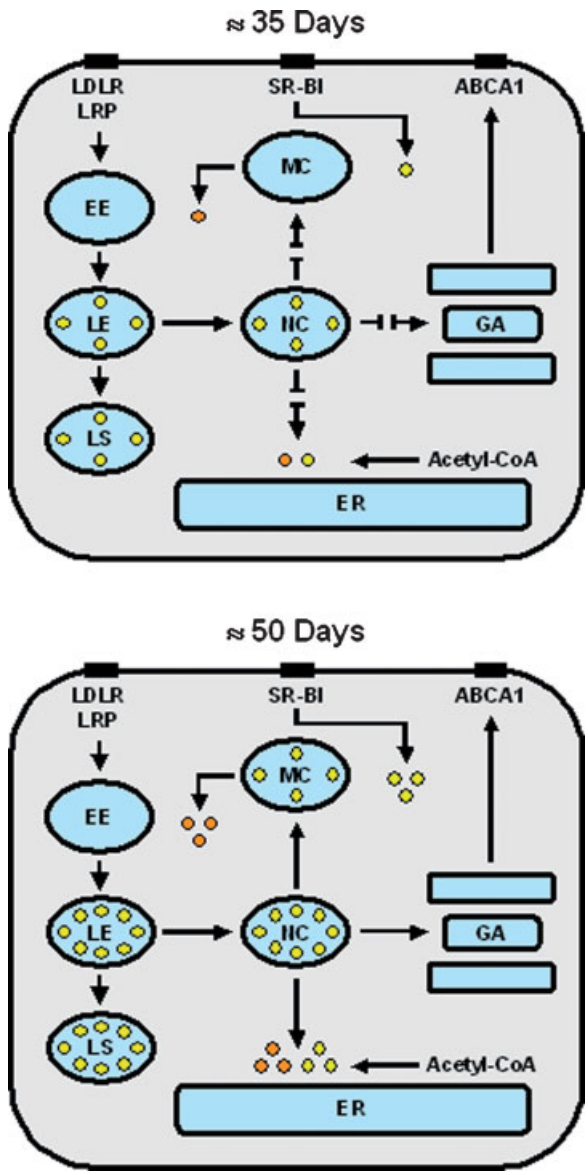

Fig. 8. The time-dependent accumulation of lipoprotein-derived cholesterol through the coated-pit pathway and proposed cellular pathophysiology associated with NPC1 liver disease. Total cholesterol that is carried in certain lipoproteins (chylomicron remnants, VLDL remnants, LDL) is internalized into early endosomes (EE) by either the low density lipoprotein receptor (LDLR) or the LRP that resides on the cell surface. The subsequent fusion of EE with late endosomes (LE) and lysosomes (LS) promotes the hydrolysis of lipoprotein-derived cholesteryl ester catalyzed by an aCEH to produce cholesterol (yellow dots). The NPC1 protein, primarily associated with the NPC1 compartment (NC) that transiently interacts with LE/LS, regulates the transport of cholesterol from LE/LS to other cellular compartments, namely mitochondria (MC) for production of oxysterols (orange dots), Golgi apparatus (GA) for redistribution of cholesterol to the plasma membrane, and the metabolically active pool of cholesterol located at the endoplasmic reticulum (ER). Mutation of the NPC1 gene and decreased NPC1 protein function results in a time-dependent accumulation of lipoprotein-derived cholesterol within LE/LS and NC. The present report suggests that NPC1$^{-/-}$ mouse hepatocytes at approximately 35 days of age have a modest increase in the amount of lipoprotein-derived cholesterol within LE/LS and NC, in addition to a relative deficiency of cholesterol that is accessible to the metabolically active pool of cholesterol (**top diagram**). However, other studies suggest that NPC1$^{-/-}$ mouse hepatocytes at approximately 50 days of age have a much larger increase in the amount of lipoprotein-derived cholesterol within LE/LS and NC, in addition to a relative excess of cholesterol that is accessible to the metabolically active pool of cholesterol (**bottom diagram**).

nalized into early endosomes by either the LDLR or LRP that resides on the cell surface [Xie et al., 1999a,b]. The subsequent fusion of early endosomes with late endosomes/lysosomes promotes the hydrolysis of lipoprotein-derived cholesteryl ester catalyzed by an acidic cholesteryl ester hydrolase (aCEH) to produce cholesterol [Goldstein et al., 1975; Anderson et al., 1977]. The NPC1 protein, primarily associated with the NPC1 compartment and late endosomes/lysosomes, has been shown to regulate the transport of cholesterol from late endosomes/lysosomes to other cellular compartments, namely mitochondria for production of oxysterols, Golgi apparatus for redistribution of cholesterol to the plasma membrane, and the metabolically active pool of cholesterol located at the endoplasmic reticulum [Blanchette-Mackie et al., 1988; Neufeld et al., 1996; Underwood et al., 1998; Zhang et al., 2002; Frolov et al., 2003]. As a result, mutation of the NPC1 gene and decreased NPC1 protein function results in the accumulation of lipoprotein-derived cholesterol in late endosomes/lysosomes and the NPC1 compartment [Pentchev et al., 1980; Liscum et al., 1989]. Importantly, studies conducted in vitro using cultured cells have indicated that decreased NPC1 protein function interferes with the production of oxysterols, while studies conducted in vivo using the NPC1 mouse indicate that an increased synthesis of endogenous cholesterol and internalization of HDL-derived cholesteryl ester through the scavenger receptor-type B, class I (SR-BI) pathway fully compensates for cholesterol sequestered in late endosomes/lysosomes and NPC1 compartment, thereby providing cholesterol to mitochondria and the endoplasmic reticulum [Xie et al., 2000b, 2006; Amigo et al., 2002; Frolov et al., 2003]. Nonetheless, it is proposed that continual sequestration of lipoprotein-derived cholesterol within late endosomes/lysosomes of $NPC1^{-/-}$ mouse hepatocytes may eventually be responsible for causing organelle damage and destabilization, resulting in the unregulated release of cholesterol/oxysterol to other cellular compartments involved in maintaining intracellular cholesterol homeostasis.

In conclusion, these studies provide an in depth investigation of liver disease and lipoprotein metabolism in $NPC1^{+/-}$ and $NPC1^{-/-}$ mice at 35 days of age. This age of mouse represented a unique time point between recovery from transient cholestasis and the onset of severe chronic liver disease characterized by elevated liver enzymes and apoptosis-mediated cell death. Together, the combined information from these studies further support the hypothesis that an accumulation of lipoprotein-derived cholesterol within late endosomes/lysosomes, in addition to altered intracellular cholesterol homeostasis, has a key role in the biochemical and cellular pathophysiology associated with NPC1 liver disease.

ACKNOWLEDGMENTS

We would like to express our most sincere appreciation to Dr. Robert P. Erickson, Diana W. Strnatka, Elizabeth S. Chaitkin, and Diana Acuna of the Genetically Modified Mouse Shared Service in the Department of Pediatrics at the University of Arizona for maintenance and genotype analysis of the Niemann-Pick C1 mice.

REFERENCES

Amigo L, Mendoza H, Castro J, Quinones V, Miquel JF, Zanlungo S. 2002. Relevance of Niemann-Pick type C1 protein expression in controlling plasma cholesterol and biliary lipid secretion in mice. Hepatology 36:819–828.

Anderson RG, Brown MS, Goldstein JL. 1977. Role of the coated endocytic vesicle in the uptake of receptor-bound low density lipoprotein in human fibroblasts. Cell 10: 351–364.

Ashkenazi A, Yarom R, Gutman A, Abrahamov A, Russell A. 1971. Niemann-Pick disease and giant cell transformation of the liver. Acta Paediatr Scand 60:285–294.

Basso F, Freeman L, Knapper CL, Remaley A, Stonik J, Neufeld EB, Tansey T, Amar MJA, Fruchart-Najib J, Duverger N, Santamarina-Fojo S, Brewer HB. 2003. Role of the hepatic ABCA1 transporter in modulating intrahepatic cholesterol and plasma HDL cholesterol concentrations. J Lipid Res 44:296–302.

Beltroy EP, Richardson JA, Horton JD, Turley SD, Dietschy JM. 2005. Cholesterol accumulation and liver cell death in mice with Niemann-Pick type C disease. Hepatology 42:886–893.

Blanchette-Mackie EJ, Dwyer NK, Amende LM, Kruth HS, Butler JD, Sokol J, Comly ME, Vanier MT, August JT, Brady RO, Pentchev PG. 1988. Type C Niemann-Pick disease: Low density lipoprotein uptake is associated with premature cholesterol accumulation in the Golgi complex and excessive cholesterol storage in lysosomes. J Biol Chem 85:8022–8026.

Camus MC, Chapman MJ, Forgez P, Laplaud PM. 1983. Distribution and characterization of the serum lipoproteins and apoproteins in the mouse, Mus musculus. J Lipid Res 24:1210–1228.

Carstea ED, Morris JA, Coleman KG, Loftus SK, Zhang D, Cummings C, Gu J, Rosenfeld MA, Pavan WJ, Krizman

DB, Nagle J, Polymeropoulos MH, Sturley SL, Ioannou YA, Higgins ME, Comly M, Cooney A, Brown A, Kaneski CR, Blanchette-Mackie EJ, Dwyer NK, Neufeld EB, Chang TY, Liscum L, Tagle DA, Strauss JF III, Ohno K, Zeigler M, Carmi R, Sokol J, Markie D, O'Neill RR, van Diggelen OP, Elleder M, Patterson MC, Brady RO, Vanier MT, Pentchev PG, Tagle DA. 1997. Niemann-Pick C1 disease gene: Homology to mediators of cholesterol homeostasis. Science 277:228–231.

Chen W, Sun Y, Welch C, Gorelik A, Leventhal AR, Tabas I, Tall AR. 2001. Preferential ATP-binding cassette transporter AI-mediated cholesterol efflux from late endosomes/lysosomes. J Biol Chem 276:43564–43569.

Choi HY, Karten B, Chan T, Vance JE, Greer WL, Heidenreich RA, Garver WS, Francis GA. 2003. Impaired ABCA1-dependent lipid efflux and hypoalphalipoproteinemia in human Niemann-Pick type C disease. J Biol Chem 278:32569–32577.

Chung BH, Wilkinson T, Greer JC, Segrest JP. 1980. Preparative and quantitative isolation of plasma lipoproteins: Rapid, single discontinuous density gradient ultracentrifugation in a vertical rotor. J Lipid Res 21: 284–291.

Chung BH, Segrest JP, Cone JT, Pfau J, Geer JC, Duncan LA. 1981. High resolution plasma lipoprotein cholesterol profiles by a rapid, high volume semi-automated method. J Lipid Res 22:1003–1014.

Clark JM, Brancati FL, Diehl AM. 2002. Nonalcoholic fatty liver disease. Gastroenterology 122:1649–1657.

Davies JP, Ioannou YA. 2000. Topological analysis of Niemann-Pick C1 protein reveals that the membrane orientation of the putative sterol-sensing domain is identical to those of 3-hydroxy-3-methylglutaryl-CoA reductase and sterol regulatory element binding protein cleavage-activating protein. J Biol Chem 275:24367–24374.

De Silva HV, Mas-Oliva J, Taylor JM, Mahley RW. 1994. Identification of apolipoprotein B-100 low density lipoproteins, apolipoprotein B-48 remnants, and apolipoprotein E-rich high density lipoproteins in the mouse. J Lipid Res 35:1297–1310.

Dietschy JM, Turley SD. 2002. Control of cholesterol turnover in the mouse. J Biol Chem 277:3801–3804.

Dietschy JM, Turley SD. 2004. Cholesterol metabolism in the central nervous system during early development and in the mature mouse. J Lipid Res 45:1375–1397.

Dietschy JM, Turley SD, Spady DK. 1993. Role of liver in the maintenance of cholesterol and low density lipoprotein homeostasis in different animal species, including humans. J Lipid Res 34:1637–1659.

Erickson RP, Garver WS, Camargo F, Hossain GS, Heidenreich RA. 2000. Pharmacological and genetic modifications of somatic cholesterol do not substantially alter the course of CNS disease in Niemann-Pick C mice. J Inher Metab Dis 23:54–62.

Erickson RP, Kiela M, Garver WS, Krishnan K, Heidenreich RA. 2001. Cholesterol signaling at the endoplasmic reticulum occurs in NPC1$^{-/-}$ but not in NPC1$^{-/-}$, LDLR$^{-/-}$ mice. Biochem Biophys Res Comm 284:326–330.

Erickson RP, Bhattacharyya A, Hunter RJ, Heidenreich RA, Cherrington NJ. 2005. Liver disease with altered bile acid transport in Niemann-Pick C mice on a high-fat, 1% cholesterol diet. Am J Phys 289:G300–G307.

Frolov A, Zielinski SE, Crowley JR, Dudley-Rucker N, Schaffer JE, Ory DS. 2003. NPC1 and NPC2 regulate cellular cholesterol homeostasis through generation of low density lipoprotein cholesterol-derived oxysterols. J Biol Chem 278:25517–25525.

Garver WS, Heidenreich RA, Erickson RP, Thomas MA, Wilson JM. 2000. Localization of the murine Niemann-Pick C1 protein to two distinct intracellular compartments. J Lipid Res 41:673–687.

Garver WS, Krishnan K, Gallagos JR, Michikawa M, Francis GA, Heidenreich RA. 2002. Niemann-Pick C1 protein regulates cholesterol transport to the *trans*-Golgi network and plasma membrane caveolae. J Lipid Res 43:579–589.

Garver WS, Xie C, Repa JJ, Turley SD, Dietschy JM. 2005. Niemann-Pick C1 expression is not regulated by the amount of cholesterol flowing through cells in the mouse. J Lipid Res 46:1745–1754.

Goldstein JL, Dana SE, Faust JR, Beaudet AL, Brown MS. 1975. Role of lysosomal acid lipase in the metabolism of plasma low density lipoprotein. Observations in cultured fibroblasts from a patient with cholesteryl ester storage disease. J Biol Chem 250:8487–8495.

Guo Q, Kohen Avramoglu R, Adeli K. 2005. Intestinal assembly and secretion of highly dense/lipid-poor apolipoprotein B48-containing lipoprotein particles in the fasting state: Evidence for induction by insulin resistance and exogenous fatty acids. Metabolism 54:689–697.

Haghpassand M, Bourassa PAK, Francone OL, Aiella RJ. 2001. Monocyte/macrophage expression of ABCA1 has minimal contribution to plasma HDL levels. J Clin Invest 108:1315–1320.

Heidenreich RA, Garver WS. 2003. The expression and function of ABCA1 is increased in livers of NPC1 mice. J Inherit Metab Dis 26:139.

Heider JG, Boyett RL. 1978. The picomole determination of free and total cholesterol in cells in culture. J Lipid Res 19:514–518.

Huang Z, Hou Q, Cheung NS, Li QT. 2006. Neuronal cell death caused by inhibition of intracellular cholesterol trafficking is caspase dependent and associated with activation of the mitochondrial apoptosis pathway. J Neurochem 97:280–291.

Ivemark BI, Svennerholm L, Thoren C, Tunell R. 1963. Niemann-Pick disease in infancy: Report of two siblings with clinical, histological and chemical studies. Acta Paediatrica 52:391–404.

Jaeken J, Proesmans W, Eggermont E, Van Hoof F, Den Tandt W, Standaert L, Van Herck G, Corbeel L. 1980. Niemann-Pick type C disease and early cholestasis in three brothers. Acta Paediatr Belg 33:43–46.

Kelly DA, Portmann B, Mowat AP, Sherlock S, Lake BD. 1993. Niemann-Pick disease type C: Diagnosis and outcome in children, with particular reference to liver disease. J Pediatr 123:242–247.

Laemmli UK. 1970. Cleavage of structural proteins during the assembly of the head of bacteriophage T4. Nature 227:680–685.

Li X, Catalina F, Grundy SM, Patel S. 1996. Method to measure apolipoprotein B-48 and B-100 secretion rates in an individual mouse: Evidence for a very rapid turnover of VLDL and preferential removal of B-48 relative to B-100 containing lipoproteins. J Lipid Res 37:210–220.

Li H, Repa JJ, Valasek MA, Beltroy EP, Turley SD, German DC, Dietschy JM. 2005. Molecular, anatomical, and biochemical events associated with neurodegeneration in mice with Niemann-Pick type C disease. J Neuropath Exp Neurol 64:323–333.

Liscum L, Ruggiero RM, Faust JR. 1989. The intracellular transport of low density lipoprotein-derived cholesterol is defective in Niemann-Pick type C fibroblasts. J Cell Biol 108:1625–1636.

Loftus SK, Morris JA, Carstea ED, Gu JZ, Cummings C, Brown A, Ellison J, Ohno K, Rosenfeld MA, Tagle DA, Pentchev PG, Pavan WJ. 1997. Murine model of Niemann-Pick C disease: Mutation in a cholesterol homeostasis gene. Science 277:232–235.

Longo M, Crosignani A, Battezzati PM, Squarcia Giussani C, Invernizzi P, Zuin M, Podda M. 2002. Hyperlipidemic state and cardiovascular risk in primary biliary cirrhosis. Gut 51:265–269.

Neufeld EB, Cooney AM, Pitha J, Dawidowicz EA, Dwyer NK, Pentchev PG, Blanchette-Mackie EJ. 1996. Intracellular trafficking of cholesterol monitored with a cyclodextrin. J Biol Chem 271:21604–21613.

Neufeld EB, Wastney M, Patel S, Suresh S, Conney AM, Dwyer NK, Roff CF, Ohno K, Morris JA, Carstea ED, Incardona JP, Strauss JF III, Vanier MT, Patterson MC, Brady RO, Pentchev PG, Blanchette-Mackie EJ. 1999. The Niemann-Pick C1 protein resides in a vesicular compartment linked to retrograde transport of multiple lysosomal cargo. J Biol Chem 274:9627–9635.

O'Kane MJ, Lynch PL, Callender ME, Trimble ER. 1997. Abnormalities of serum apoAI containing lipoprotein particles in patients with primary biliary cirrhosis. Atherosclerosis 131:203–210.

Osono Y, Woollett LA, Herz J, Dietschy JM. 1995. Role of the low density lipoprotein receptor in the flux of cholesterol through the plasma and across the tissues of the mouse. J Clin Invest 95:1124–1132.

Osono Y, Woollett LA, Marotti KR, Melchior GW, Dietschy JM. 1996. Centripetal cholesterol flux from extrahepatic organs to the liver is independent of the concentration of high density lipoprotein-cholesterol in plasma. Proc Natl Acad Sci USA 93:4114–4119.

Park WD, O'Brien JF, Lundquist PA, Kraft DL, Vockley CW, Karnes PS, Patterson MC, Snow K. 2003. Identification of 58 novel mutations in Niemann-Pick disease type C: Correlation with biochemical phenotype and importance of PTC1-like domains in NPC1. Hum Mutation 22:313–325.

Passeggio J, Liscum L. 2005. Flux of fatty acids through NPC1 lysosomes. J Biol Chem 280:10333–10339.

Patterson MC, Vanier MT, Suzuki K, Morris JA, Carstea ED, Neufeld EB, Blanchette-Mackie EJ, Pentchev PG. 2001. Niemann-Pick disease type C: A lipid trafficking disorder. In: Scriver CR, Beaudet AL, Sly WS, Valle D, editors. The Metabolic and Molecular Basis of Inherited Disease. New York: McGraw-Hill, pp 3611–3633.

Pentchev PG, Gal AE, Boothe AD, Omodeo-Sale F, Fouks J, Neumeyer BA, Quirk JM, Dawson G, Brady RO. 1980. A lysosomal storage disorder in mice characterized by a dual deficiency of sphingomyelinase and glucocerebrosidase. Biochim Biophys Acta 619:669–679.

Pentchev PG, Boothe AD, Kruth HS, Weintroub H, Stivers J, Brady RO. 1984. A genetic storage disorder in BALB/C mice with a metabolic block in esterification of exogenous cholesterol. J Biol Chem 259:5784–5791.

Pentchev PG, Comly ME, Kruth HS, Vanier MT, Wenger DA, Patel S, Brady RO. 1985. A defect in cholesterol esterification in Niemann-Pick disease (type C) patients. Proc Natl Acad Sci USA 82:8247–8251.

Pentchev PG, Comly ME, Kruth HS, Patel S, Proestel M, Weintroub H. 1986. The cholesterol storage disorder of the mutant BALB/c mouse: A primary genetic lesion closely linked to defective esterification of exogenously derived cholesterol and its relationship to human type C Niemann-Pick disease. J Biol Chem 261:2772–2777.

Rutledge JC. 1989. Progressive neonatal liver failure due to type C Niemann-Pick disease. Pediatr Pathol 9:779–784.

Schiffmann R. 1996. Niemann-Pick disease type C: From bench to bedside. JAMA 276:561–564.

Semeraro LA, Riely CA, Kolodny EH, Dickerson GR, Gryboski JD. 1986. Niemann-Pick variant lipidosis presenting as "Neonatal Hepatitis". J Pediatr Gastroenterol Nutr 5:492–500.

Sun X, Marks DL, Park WD, Wheatley CL, Puri V, O'Brien JF, Kraft DL, Lundquist PA, Patterson MC, Pagano RE, Snow K. 2001. Niemann-Pick C variant detection by altered sphingolipid trafficking and correlation with mutations within a specific domain of NPC1. Am J Hum Genet 68:1361–1372.

Tsujita M, Wu CA, Abe-Dohmae S, Usui S, Okazaki M, Yokoyama S. 2005. On the hepatic mechanism of HDL assembly by the ABCA1/apoA-I pathway. J Lipid Res 46:154–162.

Turley SD, Dietschy JM. 1988. The metabolism and excretion of cholesterol by the liver. In: Arias IM, Jakoby WB, Popper H, Schachter D, Shafritz DA, editors. The Liver: Biology and Pathology. New York: Raven Press, pp 617–641.

Turley SD, Spady DK, Dietschy JM. 1995. Role of liver in the synthesis of cholesterol and the clearance of low density lipoproteins in the cynomolgus monkey. J Lipid Res 36:67–79.

Underwood KW, Jacobs NL, Howley A, Liscum L. 1998. Evidence for a cholesterol transport pathway from lysosomes to endoplasmic reticulum that is independent of the plasma membrane. J Biol Chem 273:4266–4274.

Watari H, Blanchette-Mackie EJ, Dwyer NK, Watari M, Neufeld EB, Patel S, Pentchev PG, Strauss JF III. 1999. Mutations in the leucine zipper motif and sterol-sensing domain inactivate the Niemann-Pick C1 glycoprotein. J Biol Chem 274:21861–21866.

Wojtanik KM, Liscum L. 2003. The transport of low density lipoprotein-derived cholesterol to the plasma membrane is defective in NPC1 cells. J Biol Chem 278:14850–14856.

Xie C, Turley SD, Dietschy JM. 1999a. Cholesterol accumulation in tissues of the Niemann-Pick type C mouse is determined by the rate of lipoprotein-cholesterol uptake through the coated-pit pathway in each organ. Proc Natl Acad Sci USA 96:11992–11997.

Xie C, Turley SD, Pentchev PG, Dietschy JM. 1999b. Cholesterol balance and metabolism in mice with loss of function of Niemann-Pick C protein. Am J Phys 276: E336–E344.

Xie C, Burns DK, Turley SD, Dietschy JM. 2000a. Cholesterol is sequestered in the brains of mice with Niemann-Pick type C disease but turnover is increased. J Neuropath Exper Neurol 59:1106–1117.

Xie C, Turley SD, Dietschy JM. 2000b. Centripetal cholesterol flow from the extrahepatic organs through the liver is normal in mice with mutated Niemann-Pick type C protein (NPC1). J Lipid Res 41:1278–1289.

Xie C, Richardson JA, Turley SD, Dietschy JM. 2006. Cholesterol substrate pools and steroid hormone levels are normal in the face of mutational inactivation of NPC1 protein. J Lipid Res 47:953–963.

Yerushalmi B, Sokol RJ, Narkewicz MR, Smith D, Ashmead JW, Wenger DA. 2002. Niemann-Pick disease type C in neonatal cholestasis at a North American center. J Pediatr Gastroenterol Nutr 35:44–50.

Yu W, Gong JS, Ko M, Garver WS, Yanagisawa K, Michikawa M. 2005. Altered cholesterol metabolism in Niemann-Pick type C1 mouse brains affects mitochondria function. J Biol Chem 280:11731–11739.

Yuan XM, Li W, Olsson AG, Brunk UT. 1997. The toxicity to macrophages of oxidized low density lipoprotein is mediated through lysosomal damage. Atherosclerosis 133:153–161.

Yuan XM, Li W, Brunk UT, Dalen H, Chang YH, Sevanian A. 2000. Lysosomal destabilization during macrophage damage induced by cholesterol oxidation products. Free Radic Biol Med 28:208–218.

Zhang M, Liu P, Dwyer NK, Christenson LK, Fujimoto T, Martinez F, Comly M, Hanover JA, Blanchette Mackie EJ, Strauss JF III. 2002. MLN64 mediates mobilization of lysosomal cholesterol to steroidogenic mitochondria. J Biol Chem 277:33300–33310.